# Bifurcation and hysteresis of the magnetospheric structure with a varying southward IMF: Field topology and global three-dimensional full particle simulations

Dongsheng Cai, Weifeng Tao, Xiaoyang Yan, Bertrand Lembège, Ken-Ichi Nishikawa

# Bifurcation and hysteresis of the magnetospheric structure with a varying southward IMF: Field topology and global three-dimensional full particle simulations

DongSheng Cai,[1] Weifeng Tao,[1] Xiaoyang Yan,[1] Bertrand Lembege,[2] and Ken-Ichi Nishikawa[3]

Received 7 October 2007; revised 1 May 2009; accepted 3 August 2009; published 11 December 2009.

[1] Using a three-dimensional full electromagnetic particle model, we have performed global simulations of the interaction between the solar wind and the terrestrial magnetosphere and have investigated its asymptotic stability. The distance between the dayside magnetopause subsolar point and the Earth center, $R_{mp}$, is measured, as the intensity of southward interplanetary magnetic field (IMF) $|B_z|$ is slowly varying. Based on the field topology theory, one analyzes the variation of $R_{mp}$ as a reference index of the dynamics of this interaction, when IMF $|B_z|$ successively increases and decreases to its original value. Two striking results are observed. First, as the IMF $|B_z|$ increases above a critical value, the variation of $R_{mp}$ suddenly changes (the so-called bifurcation process in field topology). Above this critical value, the overall magnetic field topology changes drastically and is identified as being the signature of magnetic reconnection at the dayside magnetopause region. Second, this subsolar point recovers its original location $R_{mp}$ by following different paths as the IMF $|B_z|$ value successively increases from zero to a maximum fixed value and decreases from this maximum to zero while passing through some critical values. These different paths are the signature of a hysteresis effect and are characteristic of the so-called subcritical-type bifurcation. This hysteresis signature indicates that dissipation processes take place via an energy transfer from the solar wind to the magnetosphere by some irreversible way, which leads to a drastic change in the magnetospheric field topology. This hysteresis is interpreted herein as a consequence of the change of the magnetospheric field topology, or magnetic reconnection taking place at the dayside magnetopause. Sometimes, this is also called bifurcation in the nonlinear theory. The field topology reveals itself to be a very powerful tool to analyze (1) the signatures of three-dimensional magnetic reconnection without the obligation for determining the responsible mechanisms and (2) the consequences of reconnection on the overall magnetospheric dynamics.

**Citation:** Cai, D., W. Tao, X. Yan, B. Lembege, and K.-I. Nishikawa (2009), Bifurcation and hysteresis of the magnetospheric structure with a varying southward IMF: Field topology and global three-dimensional full particle simulations, *J. Geophys. Res.*, *114*, A12210, doi:10.1029/2007JA012863.

## 1. Introduction

[2] The energy transfers from the solar wind to the Earth magnetosphere, and the causes of magnetic substorms have been analyzed for decades. Axford proposed that the reconnection of magnetic fields at the dayside magnetopause is one of the candidates to explain this huge energy transfer [*Axford*, 2002; *Priest and Forbes*, 2000]. However, despite many important efforts, the mechanisms of three-dimensional magnetic reconnection and the resulting energy partition during the transfer have not been well understood within a global approach of magnetospheric dynamics. In the present paper, we investigate both the impacts and dynamics of a slowly varying southward interplanetary magnetic field (IMF) $|B_z|$ on the dayside magnetosphere in terms of bifurcation and evidence of dissipative processes [*Guckenheim and Holmes*, 1983; *Nicolis and Prigogine*, 1977, 1989; *Prigogine*, 1980; *Strogatz*, 1994; *Tobak and Peake*, 1982; *Wiggins et al.*, 2003] by using a global three-dimensional full-particle electromagnetic particle model (EMPM) in the framework of field topology theory [*Cai et al.*, 2001, 2006a]. Based on the field topology and nonlinear theory [*Guckenheim and Holmes*, 1983; *Nicolis and Prigogine*, 1977, 1989; *Prigogine*, 1980;

[1]Department of Computer Sciences, University of Tsukuba, Tsukuba, Japan.
[2]LATMOS, UVSQ, IPSL, Velizy, France.
[3]National Space Science and Technology Center, Huntsville, Alabama, USA.


0148-0227/09/2007JA012863

*Strogatz*, 1994; *Tobak and Peake*, 1982; *Wiggins et al.*, 2003], the magnetospheric magnetic field system is considered as an open system and the amplitude of the IMF $|B_z|$ is considered as the control parameter that leads the open system from the stable to unstable state. Increasing $|B_z|$ from zero to a certain value, which we call a critical value, very slowly, the open system will try to stay in the same field topology absorbing the excess energy from the solar wind at first. Exceeding this value, the system will no longer be able to absorb the excess energy, will be unstable, and will transit into a new state. Such a transition will always be accompanied by the global change of magnetospheric field topologies and thus is referred as the bifurcation in the nonlinear theory. The stability discussed here is also denoted by the term structural stability in nonlinear sciences.

[3] At the present time, our understanding of the three-dimensional magnetospheric dynamics relies principally on local observations drawn from satellites, laboratory plasma experiments, MHD and kinetic theories, and MHD, hybrid, and particle simulations. The three-dimensional magnetic field topologies in the dayside magnetosphere are visualized and observed as the index of the dynamical response of the magnetosphere to the variations of IMF $|B_z|$. The field topologies are determined and visualized mathematically using the techniques of *Cai et al.* [2001, 2006a] by searching and analyzing the magnetic null points and their eigenvalues. In fact, the change of the field topologies or the bifurcations is the signature of magnetic reconnection. The change of topologies can be identified by observing the topological properties, i.e., the number of magnetic null points, their eigenvalues, their connections etc. without determining the responsible magnetic reconnection mechanisms. The general research and the history of magnetic reconnections in magnetosphere are well summarized by *Dorelli et al.* [2007]. Herein, we follow their scenario to introduce shortly its recent developments although in the present paper we only focus and discuss on the bifurcation and the associated field topology theory:

[4] 1. "Magnetic field line merging or reconnection" is defined as "the process whereby plasma flows across a surface that separates regions containing topologically different magnetic field lines" (*Vasyliunas* [1975, p. 304], as cited by *Dorelli et al.* [2007]). Two separatrix can intersect at a line which is usually named the "separator." In field topology theory, the topological properties can be uniquely determined by the numbers and the identified types of magnetic null points. The separator is defined as the line joining two or more than one magnetic null point.

[5] 2. On the other hand, "the localized breakdown of the 'frozen-in field' condition" and "the resulting changes of 'connection'" are considered to be the basics of magnetic reconnection by *Axford* [1984], as cited by *Dorelli et al.* [2007].

[6] 3. The topological properties such as magnetic null points, separatrix surfaces, separator lines, etc., in three dimensions are known to be structurally unstable in the framework we discuss above and in section 2, reaching and exceeding the critical value [*Nicolis and Prigogine*, 1977, 1989; *Sattinger*, 1973; *Strogatz*, 1994; *Wiggins et al.*, 2003]. The "structural stability" of the "plasmoid formation" process is discussed by *Hesse and Schindler* [1988] and *Schindler et al.* [1988] in different framework and concepts without introducing the bifurcation theory. They consider that the "structural stability" is "too expensive," in other words, should not play an important role in causing the magnetic reconnection and introduce a more general definition of the magnetic reconnection based on *Axford* [1984] although the term "structural stability" they used is conceptually different from the term we use in section 2. They introduced a magnetic reconnection theory in nonvanishing magnetic fields and called it the finite-B reconnection. Please note that the finite-B reconnection does not necessarily imply a change of local magnetic field topology that will be discussed in section 2.

[7] 4. The analysis of multiple 3-D magnetic null points in the magnetosphere and a global MHD simulation for magnetosphere for the northward IMF are performed by *Dorelli et al.* [2007]. They discussed the geometry of dayside "separator reconnection" with a zero dipole tilt case where the y and z components of IMF have equal magnitude. They investigated the magnetic null points in the simulation without discussing both the field topology and the bifurcation in detail. The magnetic reconnection theories with vanishing or nonvanishing magnetic field or with separators are out of the scope of the present paper because the simulation concepts, configurations, and models, and the targeted physical problems are very different from ours. In addition to these definitions, please note that the three-dimensional reconnection has been discussed in a wide range of different scenarios. For other reconnection scenarios, please see *Boozer* [2002], *Dorelli et al.* [2007], *Hesse and Schindler* [1988], *Hornig and Priest* [2003], *Linton and Antiochos* [2005], *Pontin et al.* [2007a, 2007b], and *Schindler et al.* [1988].

[8] In the present paper, only the global topology of an open system with control parameters and their infinitesimally slow variations are considered. In many open systems, the slow variations of the control parameter may lead the systems to exhibit highly nonlinear behaviors as we discuss in section 2. In addition, when the control parameter hits a certain value and is tuned to go back to its initial value, one question arises: does the system retrieve the same topological structures or not? This can only be clarified by tracking the field topologies [*Tricoche et al.*, 2002]. Among the numerous attempts to understand the magnetospheric dynamics and its response to the solar wind parameters, not many contending arguments lend themselves to the field topology theory, topological structure, structural stability [*Priest and Forbes*, 2000], and asymptotic stability [*Guckenheim and Holmes*, 1983; *Nicolis and Prigogine*, 1977, 1989; *Prigogine*, 1980; *Strogatz*, 1994; *Tobak and Peake*, 1982; *Wiggins et al.*, 2003] of the three-dimensional magnetospheric dynamics. Both structural stability and asymptotic stability will be detailed in section 2. In the present paper, we investigate the impact of a slowly varying southward interplanetary magnetic field (IMF) $|B_z|$ on the dayside magnetosphere in terms of bifurcation and evidence of dissipative processes [*Guckenheim and Holmes*, 1983; *Nicolis and Prigogine*, 1977, 1989; *Prigogine*, 1980; *Strogatz*, 1994; *Tobak and Peake*, 1982; *Wiggins et al.*, 2003] by using a global three-dimensional full-particle electromagnetic particle simulation. The use of a 3-D PIC simulation over a global scale is discussed and is justified by an extension of the present analysis on particle injection/acceleration mechanisms before and after magnetic reconnection takes place [*Cai et al.*, 2006b] The latter is a

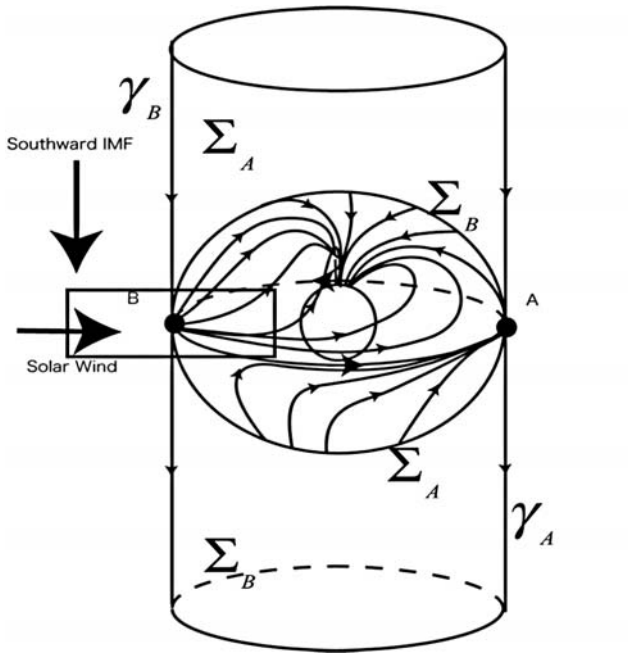


**Figure 1.** Schematic diagram of steady state mean magnetospheric field topology with highest symmetry and simplicity with a southward IMF (no perturbation is applied). This topology is an ideal one.

topic which is under active investigation. In order to discuss the dynamical problems (based on Hamiltonian), it is essential to use a numerical method like the symplectic method [*Cary and Doxas*, 1993]. However, in the present paper, we use 3-D global PIC simulation only for convenience, but we will leave the extension to the symplectic method for future work.

## 2. Field Topology, Structural Stability, and Bifurcation in Magnetospheric Dynamics

[9] The three-dimensional magnetospheric field topology and its bifurcation can be clarified when one studies how these evolve as the relevant parameters, i.e., solar wind velocity/pressure, IMF pitch angle, IMF roll angle, etc., are varying. Some of the satisfactory answers to this magnetospheric field topology question that may emerge out of the framework will be presented in this section. We will attempt to understand physical phenomena although our definitions should be treated with more purely mathematical formalism. Especially, the theory of vector field topology, topological structure, and structural stability are directly applied to investigate the properties of the magnetospheric surface magnetic field that is on the magnetopause as shown in Figure 1. Herein, we will mainly focus on the dayside. In the present section, the basic concepts of nonlinear dynamics will be introduced and reviewed.

[10] In the field topology approaches [e.g., see *Abraham and Shaw*, 1992; *Cai et al.*, 2001; *Guckenheim and Holmes*, 1983; *Tobak and Peake*, 1982; *Tricoche et al.*, 2002; *Wiggins et al.*, 2003], a pattern of magnetic field lines generates the "phase portrait" of a three-dimensional vector field. Here, we briefly introduce these field topology approaches in this section. Two "phase portraits" of the magnetic field have the same topology if a one-to-one mapping from one phase portrait to the other phase portrait preserves the paths that are magnetic field lines in the phase portrait [*Abraham and Shaw*, 1992]. We can also say in this case that two "phase portraits" are homeomorphic. Here, we consider the magnetic field as a vector field, and the paths as the magnetic field lines in the phase portrait. Let us consider a two-dimensional case and imprint a two-dimensional phase portrait on a "sheet of a rubber" that may be deformed in any way without folding or tearing. Any deformation of this sheet rubber with its associated phase portrait is a path-preserving mapping, where a magnetic field line is preserved. It is known that all characteristics of the phase portrait that remains invariant under homeomorphic mappings are represented as topological properties. They are namely (1) the number and types of magnetic null points, i.e., where the amplitude of the magnetic field is exactly zero, and are also called magnetic nulls or neutral points, (2) the existence of a path called a separator line connecting the magnetic null points, and (3) the existence of closed magnetic field lines. The types of the magnetic null points can be classified by their eigenvalues, and they are always saddles. The topological structure of the magnetic field can be characterized by the set of topological properties of the phase portrait [*Abraham and Shaw*, 1992; *Arnold*, 1973; *Cai et al.*, 2001; *Guckenheim and Holmes*, 1983; *Tobak and Peake*, 1982; *Tricoche et al.*, 2002; *Wiggins et al.*, 2003].

[11] The structural stability of a phase portrait with respect to a control parameter $\lambda$ can be defined as follows. We define a phase portrait as structurally stable for a given control parameter $\lambda$ if the phase portrait has the same topological structure as the initial one, when changing the control parameter $\lambda$ infinitesimally [*Priest and Forbes*, 2000; *Strogatz*, 1994; *Wiggins et al.*, 2003].

[12] The magnetic reconnection of the Earth's dipole magnetic field with the southward IMF has been examined by *Dungey* [1961]. In this case, the neutral line (magnetic null line) is located in the equatorial plane. For any nonzero $|B_x|$ and $|B_y|$ IMF cases that we are considering, two neutral points arise instead of the neutral line. In a global PIC simulation, finite weak, instead of zero, values of $B_x$ and $B_y$ naturally arise because of thermal fluctuations or numerical noise. As the IMF is southward, the ideal steady state magnetospheric surface magnetic field, which commonly called the magnetopause, connects to the external magnetic field via 3-D magnetic null point "A" and "B" as indicated in Figure 1 [*Lau and Finn*, 1990]. We call them 3-D negative and positive null points, respectively. By the external magnetic field, we mean the entire magnetic field including the IMF exterior to the magnetospheric surface. In a magnetic field, all magnetic null points are saddle points due to the solenoidal condition $\nabla \bullet B = 0$ [*Cai et al.*, 2001]. If one can find a path from one magnetic null point to the other, we say that the magnetic null points are connected, and we call this the null-null connections or the two 3-D null points joined by a separator [*Lau and Finn*, 1990]. Herein, the separator is the generic field line joining more than two 3-D null points [*Abraham and Shaw*, 1992; *Arnold*, 1973; *Guckenheim and Holmes*, 1983; *Tobak and Peake*, 1982; *Wiggins et al.*, 2003].

[13] In order to understand the stability of the external magnetic field that is herein the interplanetary magnetic field

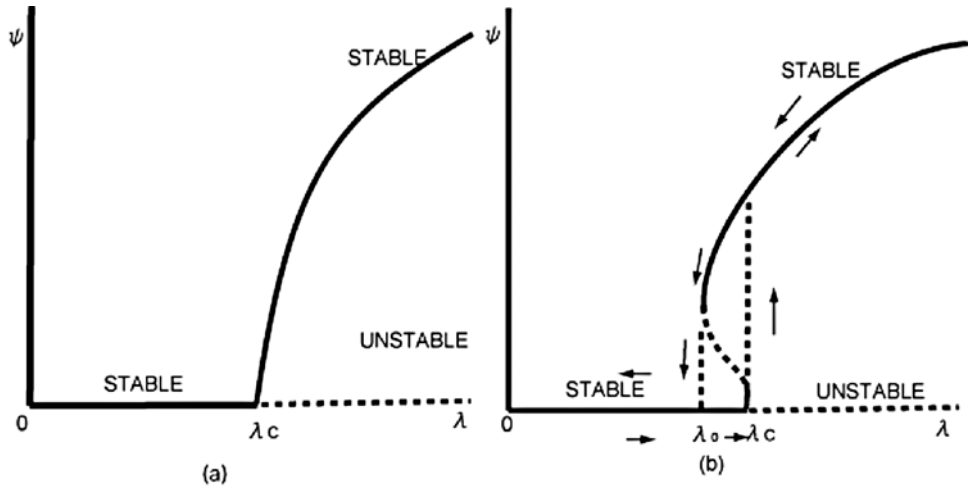


**Figure 2.** Examples of (a) supercritical or subtle bifurcation and (b) subcritical or catastrophic bifurcation. In Figure 2b the different paths followed by the arrows illustrate the hysteresis signature as $\lambda$ increases and decreases successively.

(IMF), it is necessary to properly understand the difference between structural stability and asymptotic stability of this magnetic field [*Abraham and Shaw*, 1992; *Arnold*, 1973; *Guckenheim and Holmes*, 1983; *Tobak and Peake*, 1982; *Wiggins et al.*, 2003]. First, an external magnetic field is considered structurally stable relative to a control parameter $\lambda$ if a very small change in the parameter does not alter the topological structure of the three-dimensional magnetic vector field, e. g. the number of the three-dimensional magnetic null points and the number of the positive eigenvalues of the magnetic null points. Here, the control parameter can be any parameter related to IMF or the solar wind. Second, a mean magnetic field is called asymptotically stable if small perturbations added in a given steady state, i.e., for a fixed $\lambda$, decay to zero as time $t \rightarrow \infty$.

[14] Here, we introduce the basic concepts of bifurcation and symmetry breaking [*Nicolis and Prigogine*, 1977, 1989] in conjunction with the asymptotic instability in the external magnetic field (i.e., IMF $|B_z|$). We will see these concepts may be interpreted as a signature of dissipative processes. Assume the magnetic field $B_t$ evolves according to the time-dependent equation of the general form

$$B_t = G(B, \lambda), \tag{1}$$

where $\lambda$ is a control parameter. The magnetic field evolves in time after some perturbation, i.e., change in $\lambda$, has been applied. More than one control parameters $\lambda$ can exists. However, we consider only one, for simplicity, in the present analysis. We know that solutions of $G(B, \lambda) = 0$ represent a steady state mean magnetic field that is of our interest with a given $\lambda$. Herein, we always start from this steady state mean magnetic field. The simplest mean field topology of the magnetosphere is sketched in Figure 1. As mentioned above, a mean field B is asymptotically stable, if small perturbations from it decay to zero as $t \rightarrow \infty$. When the control parameter $\lambda$ is varying, the topological structure of the mean magnetic field may be preserved or it stays as a valid solution of $G(B, \lambda) = 0$, but becomes unstable to small perturbations as $\lambda$ exceeds a critical value. At this critical point, we usually say that the known mean magnetic field is bifurcated to a new mean magnetic field. The concept just explained can be schematically sketched on a famous bifurcation diagram. Two typical examples are illustrated in Figure 2. The ordinate $\psi$ represents the known mean magnetic field that bifurcates to a new mean magnetic field, and can be any quantity characterizing the magnetic field topology. The known magnetic field becomes unstable for all values of $\lambda$ larger than $\lambda_c$, which are represented by a dashed line along the abscissa. Then, new mean magnetic fields may be bifurcated or reached from $\lambda = \lambda_c$ by two ways: the bifurcation is named supercritical or subtle (Figure 2a), and subcritical or catastrophic (Figure 2b) [*Guckenheim and Holmes*, 1983; *Nicolis and Prigogine*, 1977, 1989; *Prigogine*, 1980; *Strogatz*, 1994; *Tobak and Peake*, 1982]. Let us consider each case as follows.

[15] A supercritical bifurcation (subtle bifurcation) is shown in Figure 2a. As the control parameter $\lambda$ increases from the origin and reaches the critical value $\lambda_c$, the bifurcation occurs if the new magnetic field that takes the place of the unstable known magnetic field is changed only infinitesimally from it. Through this bifurcation, sometimes the symmetry of the known magnetic field is claimed to be broken, i.e., the magnetic field will differ as $\lambda$ increases and decreases through the critical value $\lambda_c$. Then, the magnetic field adopts a form of so-called reduced symmetry, where dissipative effects arise to absorb just the amount of excess available energy that the more symmetrical known B field was no longer able to absorb. For clarity, let us remind that theoretically, we start from the "Earth" magnetosphere under the IMF $B_z$ field in steady state. Without any perturbation, this magnetic field structure always has higher symmetry in some degree [*Nicolis and Prigogine*, 1977, 1989]. Symmetry breaking takes place where infinitesimally small perturbation acting on a system crossing a critical value $\lambda_c$, decide a system's fate, i.e., by choosing which branch of a bifurcation is taken in Figure 2 [e.g., see *Nicolis and Prigogine*, 1977, 1989].

[16] Since the bifurcation magnetic field initially evolves only infinitesimally from the unstable known magnetic field, herein the ordered magnetic field shown in Figure 1, the initial magnetospheric surface field is still kept structurally

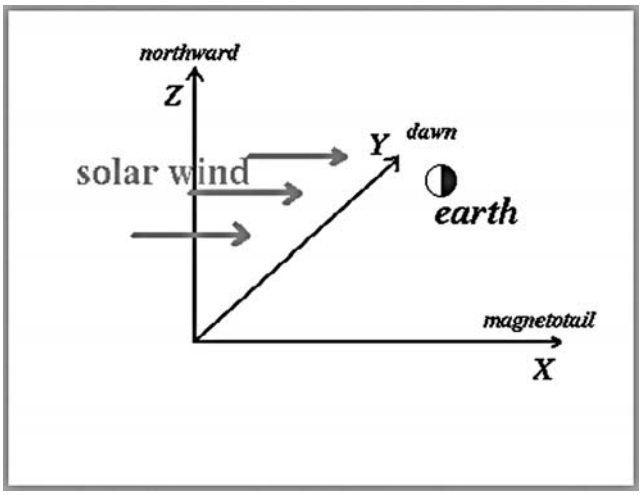


**Figure 3.** Reference set used in our 3-D PIC simulation code.

stable as $\lambda$ increases. Herein, the initial surface magnetic fields are indicated as $\Sigma_A$ and $\Sigma_B$ in the Southern and Northern Hemisphere, respectively. When $\lambda$ continues to increase crossing $\lambda_c$ (Figure 2), the new stable magnetic field varies significantly from the unstable known magnetic field, and the structural stability of the surface magnetic field begins to change. Finally, the parameter $\lambda$ reaches $\lambda_c$, at which the surface magnetic field becomes structurally unstable. This can be shown either by one of the elementary magnetic null points of its phase portrait becoming a magnetic null point that has zeros in (odd) multiple orders in Taylor expansion, or by the emergence of a new magnetic null point that has zeros in (even) multiple orders [*Sattinger*, 1973]. For clarity, let us remind the reader that the structure of the field including the spine curves and fan surface in the vicinity of the magnetic null point, where it is sufficiently close so that B is linear, can be investigated or analyzed by performing a Taylor expansion around the magnetic null points [*Buneman et al.*, 1966; *Cai et al.*, 2001; *Lau and Finn*, 1990; *Priest and Forbes*, 2000]. In either case, the magnetic null point of multiple order can be considered as being a coalescence of some elementary magnetic null points, with the equal number of positive and negative magnetic null points to satisfy the topological rule [*Priest and Forbes*, 2000; *Sattinger*, 1973].

[17] When the control parameter $\lambda$ increases just beyond the critical value $\lambda_c$, a subcritical or catastrophic bifurcation shown in Figure 2b emerges if adjacent bifurcation magnetic fields that differ only infinitesimally from the unstable known magnetic fields do not exist. Thus, a finite or catastrophic jump to a new bifurcation branch of magnetic fields occurs. This finite jump to the new branch in Figure 2b may indicate a radical change in the topological structure of the external magnetic field and in the phase portrait of the surface magnetic field as well. Sometimes this is referred to as a catastrophe. When $\lambda$ is decreased further just below $\lambda_c$, the bifurcation magnetic field does not recover the original stable magnetic field. Indeed, the stable known magnetic field appears again only when $\lambda$ is decreased far enough below $\lambda_c$ to pass through another critical value $\lambda_0$ as illustrated in Figure 2b. The difference between the two states followed by the magnetic field, as the parameter $\lambda$ increases and decreases, is the signature of the hysteresis effect. In subcritical bifurcation, the bifurcation magnetic fields will always display the hysteresis effect. However, the hysteresis effect does not always imply that the subcritical bifurcation occurs. In Figure 2b, the dashed line between $\lambda_0$ and $\lambda_c$ represents one of possible solutions of the magnetic field (unstable) in this system as $\lambda$ decreases. This part will be not discussed herein. Here, we also have to refer to the work by *Schroer et al.* [1994], where they investigated the subcritical bifurcation of a nonlinear two-dimensional current sheet using the stationary resistive-viscous MHD equations. They also investigated the secondary bifurcation in their model.

## 3. Simulation Model

[18] In our simulation, we use the same initial conditions to form the magnetosphere [*Buneman et al.*, 1980, 1992; *Buneman*, 1993], the same radiating boundary conditions [*Lindman*, 1975] and the charge-conserving formulas [*Villasenor and Buneman*, 1992] as in our previous works [*Nishikawa*, 1997, 1998; *Nishikawa and Ohtani*, 2000a, 2000b]. The simulation model is a three-dimensional electromagnetic full particle global simulation model with a reference set shown in Figure 3, where $\Delta \approx 0.5$ Re, and $\Delta t = 1$ is the time step ($\omega_{pe}\Delta t = 0.12$). Here, $\Delta = \Delta x = \Delta y = \Delta z$. Initially, we use about $36 \times 10^6$ electron-ion pairs, which corresponds to a uniform particle density of $\tilde{n} = 8$ pairs per cell across the simulation domain ($215\Delta \times 145\Delta \times 145\Delta$). The normalized physical quantities are, for electrons and ions, respectively, defined as follows: thermal velocity: $\tilde{v}_{the,i} = v_{the,i}/(\Delta/\Delta t)$; Debye length: $\lambda_{De,i} = \tilde{v}_{the,i}/\tilde{\omega}_{pe,i}$; Larmor gyroradius: $\tilde{\rho}_{ce,i} = \tilde{v}_{the,i}/\tilde{\omega}_{ce,i}$; inertia length: $\tilde{\lambda}_{ce,i} = \tilde{c}/\tilde{\omega}_{pe,i}$; gyrofrequency: $\tilde{\omega}_{ce,i} = \omega_{ce,i}\Delta t = (B\Delta m_e/\Delta t m_{e,i})$; and plasma beta: $\tilde{\beta}_{e,i} = \tilde{T}_{e,i}\tilde{\omega}^2_{pe,i}/\tilde{B}^2$. Values of normalized ambient plasma parameters used in our simulation are, for electrons and ions, respectively: $\tilde{v}_{the,i} = (0.09, 0.045)$; $\lambda_{De,i} = (0.75, 1.5)$; $\tilde{\omega}_{pe,i} = (0.125, 0.031)$; $\tilde{\omega}_{ce,i} = (0.20, 0.013)$: $\tilde{\rho}_{ce,i} = (0.45, 3.5)$; $\tilde{\lambda}_{ce,i} = (4.2,16.1)$; $\tilde{\beta}_{e,i} = (0.2, 0.8)$; and $\tilde{T}_{e,i} = (0.008, 0.032)$. Here, $\tilde{c} = 0.5$ is the speed of light. The center of the current loop that generates the dipolar terrestrial magnetic field is located at ($80\Delta$, $72.5\Delta$, $73\Delta$). Within the time range $0 < \tilde{t} < 1000\Delta\tilde{t}$ a drift velocity $\tilde{v}_{sol} = -0.5\tilde{c}$ representing the solar wind, is applied along the x direction without an IMF. The injected solar wind density has also $\tilde{n} = 8$ electron-ion pairs per cell, the mass ratio is $m_i/m_e = 16$, and the electron and ion thermal velocities are $\tilde{v}_{the} = \sqrt{\tilde{T}_e/m_e} = 0.18\tilde{c}$ and $\tilde{v}_{thi} = \sqrt{\tilde{T}_i/m_i} = 0.09\tilde{c}$ respectively.

[19] The main purpose of our global simulation is to observe the dynamic response of the magnetosphere due to the variations of IMF |Bz| as a control parameter. Moreover, we expect the irreversible kinetic effects or related microscopic phenomena will not play an important role in the determination of the topological structure of the magnetosphere. Therefore, only the interaction between macroscopic electric and magnetic field and electrons and ions, and possibly their related accelerations within a self-consistent approach are considered in the present model. Indeed, the

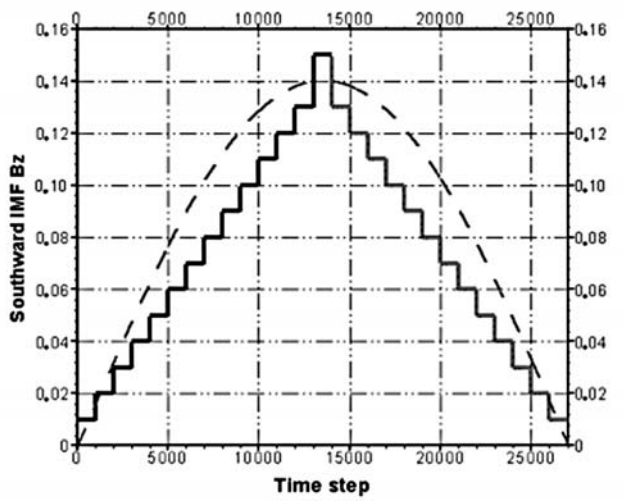


**Figure 4.** Time history of the southward IMF $|B_z|$ applied in this simulation.

minimum distance from the Earth center to the dayside magnetopause $R_{mp}$ is about 20$\Delta$ and the resolution is too coarse to simulate any kinetic instability in the present model. In this sense, our simulation model is similar to early works of particle simulations, for example [*Buneman et al.*, 1966; *Cai and Buneman*, 1992], where the stability of cross-field beams is discussed and the kinetic instabilities are not discussed. All the physical values are scaled using the minimum distance to the magnetopause ($R_{mp}$) and the solar wind velocity $V_{sw}$. If we assume $R_{mp}$ = 70,000 km and the solar wind velocity Vsw = 200–400 km/s, one grid size $\Delta$ is about 3,500 km and 1000 simulation time step corresponds to about 73–36.5 min. The thermal electron gyroradius is 0.45$\Delta$ and the electron gyro-motion may not be correctly solved. The electron plasma parameter, i.e., the number of particles within the Debye sphere, is about 14 and some particle collisional effects are expected. Thus, a smoothing techniques is applied in order to reduce the noise generated from the collisions [*Buneman et al.*, 1980, 1992; *Buneman*, 1993]. In the present model, the ionosphere model is not implemented and the particles entering into the region corresponding to the expected ionosphere are automatically taken out from the simulations. The electron and ion inertia lengths are, 4$\Delta$ and 16$\Delta$, respectively, in our simulation; thus, it is too coarse to simulate the bow shock in our simulation size. Due to the severe limitation of the computer resources, the simulation box in x, y, and z are limited and the far magnetotail region is not analyzed.

## 4. Results

[20] In the present paper, with the help of 3-D electromagnetic full particle simulation code and using the analogy with the bifurcation theory summarized in section 2, we have investigated the asymptotic stability of the interplanetary magnetic field (IMF) and the structural stability of the magnetospheric surface magnetic field at the dayside magnetopause: herein, the time-varying southward IMF is considered as an external disturbances.

[21] We will focus on the magnetic field in the dayside magnetosphere and the magnetopause region in which subcritical bifurcation is interpreted herein as a signature of large-scale dissipative processes. Let us first consider how magnetic reconnection on the magnetopause may originate on a magnetospheric surface of revolution when one of the main parameters–herein the strength of the southward IMF $|B_z|$, which plays the role of the control parameter $\lambda$ in Figure 2, is slowly varying. Let us remind that the parameter $\lambda$ in Figure 2 is supposed to designate any quantity that characterizes the magnetic field. Indeed, we focus on the changes of this magnetic field, i.e., bifurcation, during the interaction of the magnetized solar wind with the magnetosphere. Then one finds it is convenient to let the ordinate $\psi$ designate the maximum distance $R_{mp}$ of the magnetopause, since $R_{mp}$ changes significantly if the bifurcation occurs. Here, $R_{mp}$ is measured from the dayside subsolar point to the geomagnetic center, and will decrease as the control parameter, i.e., the amplitude of IMF $|B_z|$, increases. Our three-dimensional global simulation is performed as the southward IMF $|B_z|$ is varying as shown in Figure 4. The southward IMF $|B_z|$ is increased step by step from 0.0 to 0.15 within increment of 0.01. For each increment, we start from the last time of previous simulation and continuously extend the simulation for 1000 additional time steps so that the solar wind with new IMF prevails over the whole simulation domain and the overall solar wind–magnetosphere interaction reaches a "near steady state." The process is repeated until the southward IMF $|B_z|$ increases up to 0.15. Afterward, we begin to decrease IMF $|B_z|$ to zero with a decrement of 0.01 identical to the increment value. The simulation is started again and performed continuously for 1000 additional time steps for each decrement so that the solar wind with new IMF $|B_z|$ prevails in the whole simulation domain. Varying the southward IMF $|B_z|$, the complete $R_{mp}$ – IMF $|B_z|$ diagram can be

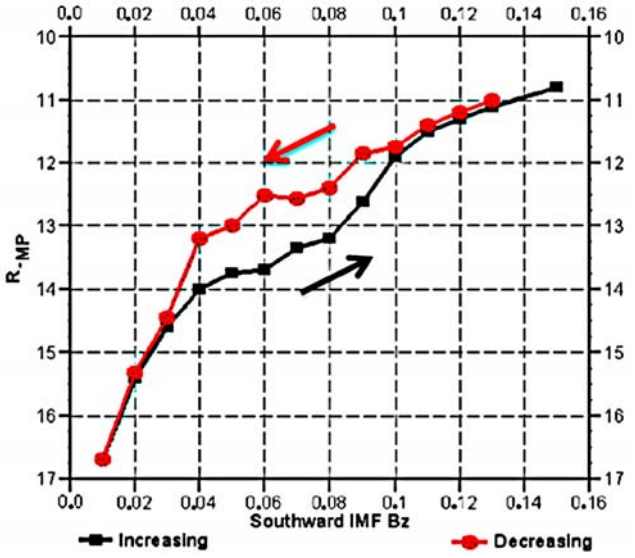


**Figure 5.** Variation of $R_{mp}$ versus the southward IMF $|B_z|$. The hysteresis signature is evidenced by the difference between the black curve (increasing southward IMF $|B_z|$) and the red curve (decreasing southward IMF $|B_z|$).

drawn and evidences hysteresis signature as displayed in Figure 5. As the strength of the southward IMF $|B_z|$ increases, $R_{mp}$ decreases (black curve), and increases as the strength of IMF $|B_z|$ decreases (red curve). The gap between the black and red curves, i.e., hysteresis, demonstrates that the magnetopause with the decreasing IMF $|B_z|$ does not recover to its initial location $R_{mp}$ in the same way with the increasing path. Indeed, within the range $0.04 < |B_z| < 0.08$, where the slope of the curve changes noticeably as IMF $|B_z|$ increases and decreases, $R_{mp}$ is smaller, i.e., pressure of the magnetospheric field is smaller, as the IMF $|B_z|$ decreases, while $R_{mp}$ is larger, i.e., the pressure of the magnetospheric field is larger, as the IMF $|B_z|$ increases. This indicates that some irreversible energy transfer from the solar wind to the magnetosphere takes place via some dissipative processes over the successive increase and decrease of IMF $|B_z|$.

[22] More exactly, as the strength of the southward IMF increases, the magnetosphere is strongly compressed on the dayside and shrinks linearly at the initial stage, where $|B_z| = 0.01$ to 0.04 and $R_{mp}$ strongly decreases. Then its location gradually stabilizes, where $|B_z| = 0.04$ to 0.08 and $R_{mp}$ weakly decreases only: the shrinking almost saturates while absorbing the excess energy from the solar wind and keeping the same topological structure. The whole stage where $|B_z| = 0.01$ to 0.08 corresponds to the stage 0 to $\lambda_c$ in the bifurcation diagram of Figure 2b, although the curve in Figure 5 is not flat due to the nature of $R_{mp}$. At that stage, one can consider that the magnetosphere can be slightly deformed without bifurcation absorbing the excess energy from the solar wind. In the final stage, the control parameter $\lambda$, i.e., IMF $|B_z|$, passes through the critical value $\lambda_c = |B_z| = 0.08$, a catastrophic-like finite up-jump of $R_{mp}$ suddenly occurs because the magnetospheric system can no longer absorb the excess energy and no adjacent magnetic field exists.

[23] After the southward IMF $|B_z|$ reached 0.15, the southward IMF decreases gradually and the magnetic field is still on the new branch of a stable field. At the first stage, as IMF $|B_z|$ varies from 0.15 to 0.08, the dayside magnetosphere progressively recovers and $R_{mp}$ decreases linearly. However, as $\lambda$ is just below $\lambda_c$, the magnetic field does not return to the original stable known magnetic field. The recovery almost saturates, when $\lambda$ is decreased far enough below $\lambda_c$ to pass through another critical value $\lambda_0 = 0.04$. A second finite down-jump of $R_{mp}$ suddenly occurs and allows to access to the stable known magnetic field which is fully recovered.

[24] In Figure 5, the finite jump is not as drastic as in Figure 2b. The reason is that for each southward IMF value the magnetic field should reach the asymptotically stable and steady state before the critical bifurcation point $\lambda_c$. However, due to the constraints of computer power and CPU time, we have to change the southward IMF value (increment/decrement) after a reasonable number of time steps (1000). Then, the perturbations or noises caused by varying $\lambda$ may still partially remain and the magnetic field dynamics is not in perfect steady state.

[25] The important point is that no artificial form of dissipation, i.e., resistivity as used in hybrid simulation, is included in our PIC simulation. However, the hysteresis signature that is clearly evidenced indicates that some dissipation processes take place in some irreversible way. The main invoked reason for this dissipation is the energy transfer from the solar wind to the magnetosphere and the emergence of the dissipative structures to be able to absorb the transferred energy or symmetry breaking at the bifurcation point.

[26] Using the analogy of the bifurcation theory introduced in section 2, as the control parameter $\lambda$, i.e., the IMF $|B_z|$, increases and passes the critical value $\lambda_c$, both the external (IMF) and the magnetospheric surface magnetic field may bifurcate into a new mean magnetic field. The subcritical bifurcation may lead to a radical change in the topological structure of the magnetic field in such a way that the symmetry of the known magnetic field is broken. This symmetry breaking in subcritical bifurcation with hysteresis is interpreted as being due to irreversible dissipation processes which absorb just the amount of excess available energy that symmetrical known magnetic field could no longer absorb. For a more comprehensive approach, our present results show that the subcritical-type bifurcation is an irreversible process while the supercritical bifurcation is a reversible process. The subcritical-type bifurcation indicates a dissipation process.

[27] The consequences on the magnetospheric field topology may be analyzed by reminding that the pressure balance between the solar wind ram pressure and the magnetospheric field pressure determines the distance $R_{mp}$ of the dayside magnetopause or subsolar point from the "Earth." As the strength of the southward IMF $|B_z|$ increases and exceeds $\lambda_c$, the magnetic reconnection, expressed herein in terms of bifurcation, takes place at the dayside magnetopause. The magnetic field and the magnetospheric surface phase portrait transit to a new stable state. Large-scale dissipative processes reach the new state and the excess energy contained in this new state can be absorbed.

[28] A more comprehensive approach may be performed with the help of field topology. Figure 1 is the schematic diagram of ideal magnetic field topology, i.e., highest symmetry with only two magnetic null points "A" and "B." In a 3-D analysis, a magnetic null point is characterized by three eigenvectors and three eigenvalues. Positive and negative magnetic null points are defined by two positive and two negative real parts of eigenvalue, respectively [*Priest and Forbes*, 2000]. The magnetospheric surface or magnetopause is covered by negative and positive fan surfaces $\Sigma_A$ and $\Sigma_B$, respectively [*Lau and Finn*, 1990; *Priest and Forbes*, 2000]. Bifurcation occurs by splitting the magnetic null points "A" and "B" following the topological rule summarized in section 2. In our simulation, due to the insufficient grid resolution, the magnetosphere has no sufficient symmetry as shown in the ideal situation of Figure 1. We have searched for a magnetic null point only in the rectangle region around the subsolar point as shown in Figure 1.

[29] Figures 6a and 6b show 2-D curves of the magnetic field that is cross section of the meridian plane Z-X for IMF $|B_z| = 0.1$, respectively, defined in the increasing and decreasing phase of the IMF (black and red curves, respectively, in Figure 5). Figures 7a–7i show three magnetic field topologies by simply visualizing the fan surfaces ($\Sigma$ surfaces) and the spine curves ($\gamma$ lines) of the magnetic null points found around the dayside region and

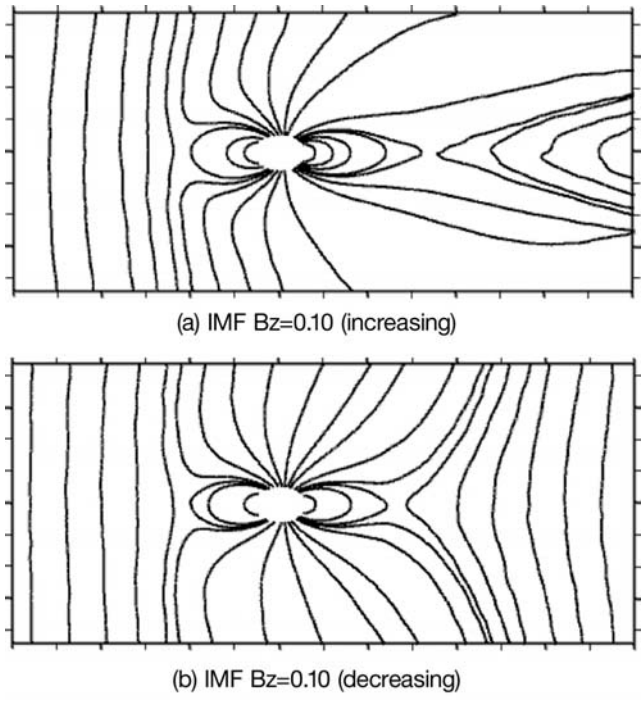


**Figure 6.** Cross section at the meridian plane Z-X of the magnetic field for IMF $|B_z| = 0.1$ defined in the (a) increasing and (b) decreasing phase of the IMF.

they are projected in the planes X-Z (Figures 7a, 7d, and 7g), X-Y (Figures 7b, 7e, and 7h), and Y-Z (Figures 7c, 7f, and 7i). Figures 7a, 7b, and 7c are defined for IMF $|B_z| = 0.08$ in the increasing phase (black curve of Figure 5), i.e., just before the catastrophic like jump, while Figures 7d, 7e, and 7f are defined for IMF $|B_z| = 0.1$ in the increasing phase (black curve of Figure 5), i.e., just after the catastrophic-like jump. Similarly, Figures 7g, 7h, and 7i are shown for IMF $|B_z| = 0.1$ in the decreasing phase (red curve of Figure 5), i.e., when IMF $|B_z|$ does not recover yet its original value. In Figures 7a–7i, all magnetic null points are saddle points. Fan surfaces ($\Sigma$ surfaces) associated to a positive and negative magnetic null point are visualized with blue and red, respectively. Spine curves ($\gamma$ lines) associated to a positive and negative magnetic null point are visualized with yellow and dark red, respectively [*Cai et al.*, 2001, 2006a]. The fan surfaces drawn in Figure 7 cover only limited regions. Due to insufficient numerical accuracy, it is difficult to extend these surfaces to larger region at present time. In addition, the fan surfaces extended from other regions, especially from the magnetotail region where magnetic reconnection is also expected, are not drawn here. Thus, the magnetospheric surfaces are only analyzed in the visualized region that is corresponding to the subsolar region.

[30] As shown in Figures 7a, 7b, and 7c defined for IMF $|B_z| = 0.08$ on the increasing black curve in Figure 5 before the bifurcation, a magnetic null point is now split into five magnetic null points including three positive and two negative magnetic null points. However, the five magnetic null points are still tightly connected and clustered around a small area near the magnetopause subsolar region illustrated by the white rectangle. These are the 3-D magnetic null points joined by separators. Comparing with Figure 1, these 3-D magnetic null points joined by separators appear by introducing two new positive-negative null pairs following the topological rule in section 2. As shown in Figures 7a, 7b, and 7c, three fan surfaces are connected to the "Earth" including two negative fan surfaces (red) and one positive (blue). Two positive fan surfaces (blue) span out to outside magnetosphere. These are the typical topological properties discussed in section 2. In order to avoid any overwhelming in Figures 7a–7c, the connecting line joining each magnetic null point is not shown.

[31] As shown in Figures 7d, 7e, and 7f, $\lambda = 0.1$, after the bifurcation, the magnetic null points are no longer tightly connected in one small region located around the subsolar point but begin to separate both duskward (−y) and dawnward (+y), and form two separated clusters illustrated now by two separate rectangles. In Figures 7d–7f, one negative-positive null pair is focused on the dawnside (+y), and two negative and one positive magnetic null points are focused on the duskside (−y). The magnetic null points illustrated by white dots may not visible in Figures 7e and 7f due to 3-D perspective representation. Instead, the white rectangles are located in the regions where the magnetic null points are clustered. In total, we have two positive and three negative magnetic null points. At the same time, they significantly move earthward (+x), the dayside magnetosphere significantly shrinks, and this causes the jump in Figure 5. In this case, the topological rule is observed by matching the magnetic null points in the tail globally. One negative (red) and positive (blue) fan surface pair in the dawnside (+y) connects to the "Earth" South and North Pole, respectively. One negative fan surface (red) in the duskside (−y) connects to the "Earth" South Pole, and one positive (blue) and negative (red) fan surface pair span out to outside magnetosphere.

[32] After $\lambda = 0.1$, we still increase $\lambda$ up to 0.15. During the increase of $\lambda$, the number of magnetic null points increases and they are divided into two groups, i.e., one in the dawnside and another in the duskside, and both move toward the flanks of magnetosphere, i.e., to $\pm y$, respectively. At the same time, each group moves backward (−x), i.e., toward the "Earth." The dayside magnetosphere continues to shrink. The two clusters are separated each other and move duskward (−y) and dawnward (+y) in opposite directions and the global separator joining them largely extends. This phenomenon is the "extension of global separator" and is the analog of the so-called "X line extension" in 2-D simulation. After $\lambda$ reaches the value 0.15, we gradually decrease $\lambda$ back to 0.1 (red). While decreasing $\lambda = 0.1$ (red curve in Figure 5), the magnetic null points are still split into two groups as shown in Figures 7g, 7h, and 7i. One group with three magnetic null points is located in the dawnside (+y) while another with two magnetic null points is located in the duskside (−y). However, these do not return to the same locations, and remain far from the subsolar point. Thus, the newly created magnetic null points, which moved outside the region represented in Figure 7, cannot be shown. A new algorithm to resolve this problem should be presented in the near future. After the bifurcation, a new magnetic field topology emerges and the new magnetic null points appear as positive-negative pairs or in even numbers, and those pairs

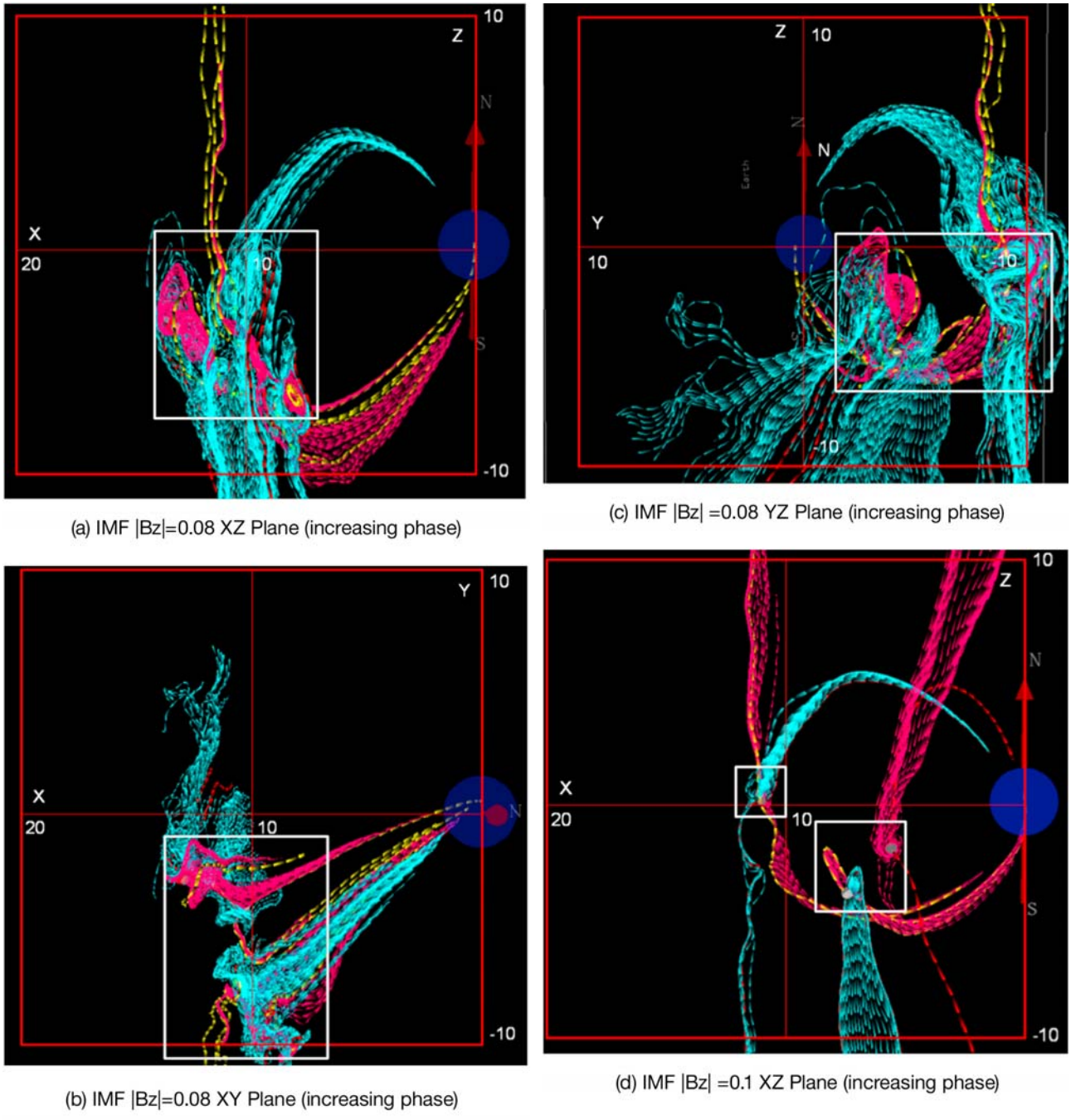


**Figure 7.** (a–c) One magnetic field topology is shown for IMF $|B_z|$ = 0.08 in the increasing phase before bifurcation. Two magnetic field topologies are shown for southward IMF $|B_z|$ = 0.1 after bifurcation as southward IMF $|B_z|$ (d–f) increases from lower values and (g–i) decreases from higher values. Magnetic field topologies are shown at the X-Z plane in Figures 7a, 7d, and 7g, at the Y-X plane in Figures 7b, 7e, and 7h, and at the Y-Z plane in Figures 7c, 7f, and 7i. The white dots are the magnetic null points. The white dots may be difficult to see due to some 3-D perspective representations, especially for Figures 7c, 7d, and 7f. Instead, white rectangles are used to focus on the regions where the magnetic null points are clustered. One initial rectangle (one cluster) defined for IMF $|B_z|$ = 0.08 is split into two rectangles (two clusters) for IMF $|B_z|$ = 0.1 for $\lambda$ increasing/decreasing phases. Fan surfaces ($\Sigma$ surfaces) associated with a positive and negative null point are visualized with blue and light red, respectively. Spine curves ($\gamma$ lines) from a positive and negative null point are visualized with yellow and dark red, respectively.

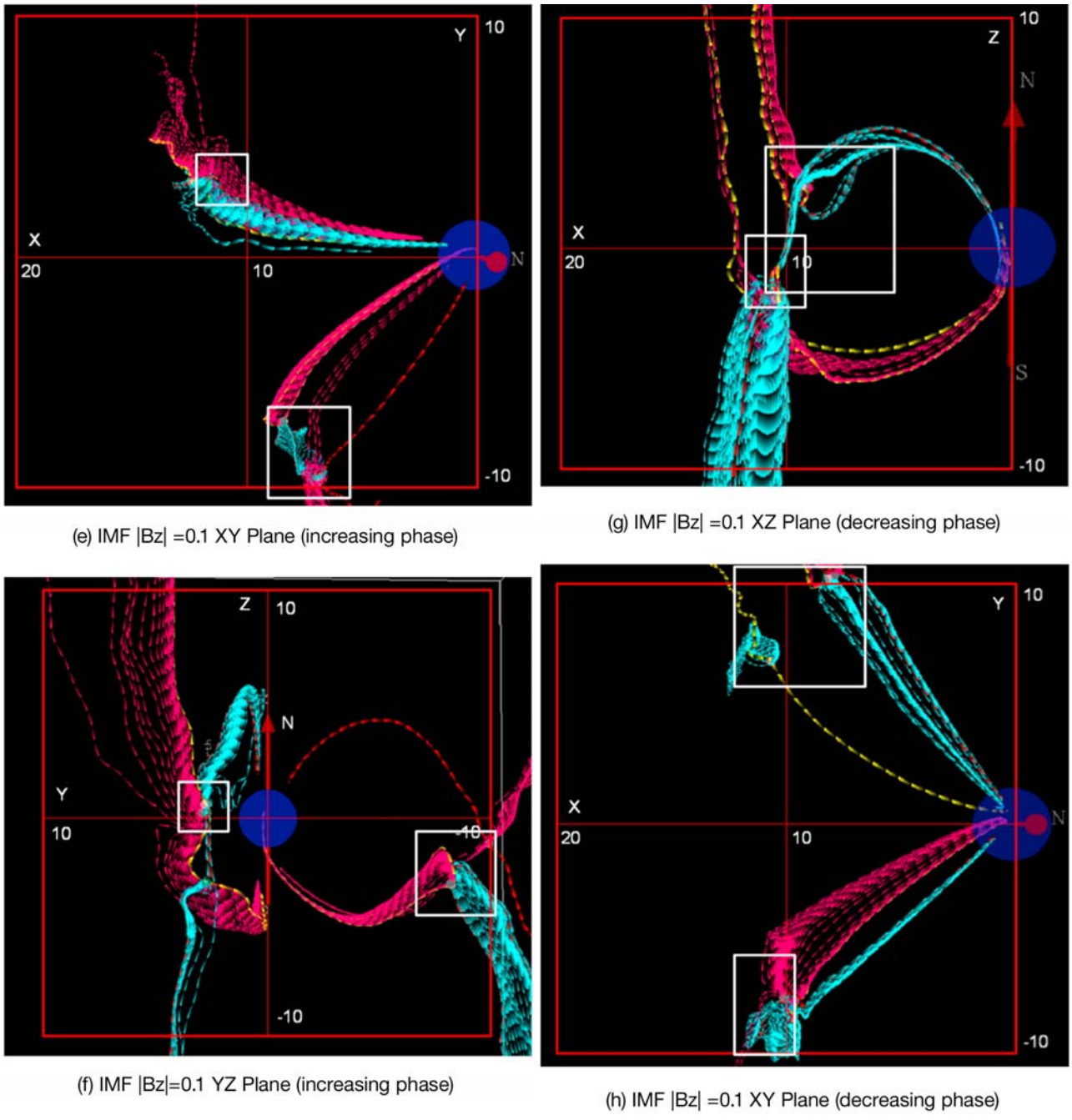


**Figure 7.** (continued)

matched with the magnetic null points in the tailside that is outside the investigated region.

[33] In summary, when the increasing $\lambda$ exceeds a certain value, shown as black curve in Figure 5, a new magnetic field topology composed of two clusters of magnetic null points in the dawnside and duskside emerge after the bifurcation, and the newly bifurcated field in the branch of a stable magnetic field stays almost unchanged. Even if we increase the $\lambda$ parameter further and decrease it back to the same point, the branch of a stable magnetic field stays unchanged. This means that the magnetic null points remain split into two clusters located in the dawnside and duskside regions, respectively. At the same time, this splitting is the key point for understanding how the bifurcated magnetospheric structure absorbs the excess energy from the solar wind. Of course, some local modifications of the topology can be found and, strictly speaking, the field topology differs among all three cases considered in Figure 7. Two topologies of the magnetic field shown in Figures 7d, 7e, and 7f and Figures 7g, 7h, and 7i are "topologically almost equivalent" because for both cases the magnetic null points are divided into two groups in dawnside and duskside, respectively. This evidences that the two groups still remain on the same branch of the magnetic field. However, the

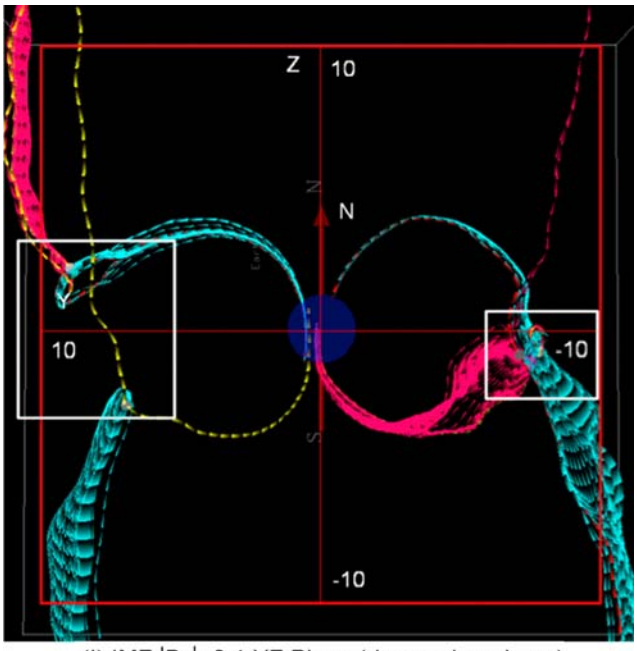


(i) IMF |Bz|=0.1 YZ Plane (decreasing phase)

**Figure 7.** (continued)

distance between the two groups of magnetic null points in Figures 7g, 7h, and 7i for $\lambda = 0.1$ (red) are 1.7 times larger than that in Figures 7d, 7e, and 7f for $\lambda = 0.1$ (black). The two groups of the magnetic null points do not return close enough to the subsolar point as $\lambda$ is approaching $\lambda_0$. This difference is the consequence of the decreasing $\lambda$ (red curves in Figure 5) exceeding the critical value $\lambda_c$. Similar differences are also found in the nearby magnetotail region but are not analyzed herein. Please note that instead of discussing the strict argument of topological equivalence, here we mainly focus on how the magnetic null points are split into two clusters of magnetic null points, because these are searched and analyzed only within the limited area of the subsolar region.

## 5. Conclusions

[34] In the present paper, we analyze the dynamics of the dayside magnetospheric region by using an analogy with the bifurcation theory based on the field topology. This analogy allows us to show that the solar wind magnetic field and the magnetospheric surface magnetic field may bifurcate as the southward IMF increases and exceeds a critical value. This is inferred by the following observations: (1) one cluster of magnetic null points near the subsolar region is split into two clusters on the dawnside and duskside, respectively, as shown in Figure 7, and a different topology appears when $\lambda$ exceeds this critical value; (2) at the same time the size of the dayside magnetosphere, or the distance $R_{mp}$, is significantly reduced. Thus, we infer that the bifurcated magnetic field that replaces the unstable known magnetic field may break the symmetry of the known field, adopting a form of reduced symmetry in which dissipative processes arise to absorb the excess energy from the solar wind. More precisely, when the parameter $\lambda$ exceeds the critical value$\lambda_c$, there may be no adjacent bifurcated magnetic field that differs only infinitesimally from the unstable known magnetic field. Instead, one may evidence a finite jump to a new branch of the field that may represent a radical change in the topology of the external magnetic field and in the phase portrait of the magnetospheric surface field in dayside as shown in Figure 7.

[35] The rigorous arguments of topological changes or bifurcation are not discussed here. In particular, the changes in the external magnetic field require further investigation which will be reported in future study [*Tricoche et al.*, 2002]. The physical mechanism of how the magnetosphere reaches the configuration where large-scale dissipative processes can take place and where 3-D topological structure allows the magnetosphere to absorb the excess energy from the solar wind is the crucial point to understand the dynamics of overall magnetosphere. However, we would like to leave this for our future research. According to the bifurcation theory discussed in section 2, this jump and the associated bifurcation are difficult to predict precisely. This subcritical type or jump-like transition is proposed to be the signature of the magnetic reconnection process at the dayside region. As the parameter $\lambda$ decreases, the magnetopause recovers its initial state but not following the same path used as $\lambda$ increases: hysteresis effect is evidenced within a certain interval of IMF $|B_z|$ values. This hysteresis is the signature of irreversible dissipation processes during which the topology of the magnetic field is strongly changed (Figure 7) and does not recover its initial state for the same value of the IMF $|B_z|$ within this interval. In other words, the field energy previously stored in the magnetosphere since IMF $|B_z|$ is increasing but is not spontaneously recovered as $\lambda$ decreases. These properties represent the indirect signatures of the reconnection process on the dayside.

[36] These features may have certainly some consequences for the Space Weather program, concerning the impact of a long-term southward IMF variation (increase/decrease) on the magnetosphere dynamics [e.g., *Nishikawa and Ohtani*, 2000a]. These may certainly present strong difficulties for the predictions in the global solar wind–Earth environment interactions. Additional points such as how the bifurcation magnetic fields break the symmetry of the known field, and what dissipative processes take place can only be understood by using the field topology analysis. However, these points are not yet addressed in the present work and are left for a future investigation.

[37] **Acknowledgments.** We thank the Solar Terrestrial Laboratory and the Information Center of Nagoya University for giving us great support and for the use of their supercomputers. We thank Glynn Germany for improving the English. K.N. is supported by NSF ATM-0100997, INT-9981508, and AST-0506719 and NASA-NNX08AG83G, NNX08AL39G, and NNX09AD16G. We also thank the Center for Computational Sciences of University of Tsukuba for letting us use the new cluster system T2K.

[38] Zuyin Pu thanks David Pontin and the other reviewers for their assistance in evaluating this paper.

## References

Abraham, R. H., and C. D. Shaw (1992), *Dynamics: Geometry of Behavior*, Addison-Wesley, New York.

Arnold, V. I. (1973), Ordinary Differential Equations, translated and edited by R. A. Silverman, MIT Press, Cambridge, Mass.

Axford, W. I. (1984), Magnetic field reconnection, in *Magnetic Reconnection in Space and Laboratory Plasmas*, *Geophys. Monogr. Ser.*, vol. 30, pp. 1–8, edited by E. W. Hones Jr., AGU, Washington, D. C.

Axford, W. I. (2002), Connection and reconnection, *Adv. Space Res.*, *29*(7), 1025–1033.

Boozer, A. H. (2002), Reconnection and the ideal evolution of magnetic fields, *Phys. Rev. Lett.*, *88*(21), 215005, doi:10.1103/PhysRevLett.88.215005.

Buneman, O. (1993), *TRISTAN: The 3-D, EM Particle Code*, *Comput. Space Plasma Phys. Simulation Tech. Softw.*, vol. 67, edited by H. Matsumoto and Y. Omura, Terra Sci., Tokyo.

Buneman, O., et al. (1966), Stability of crossed-field electron beams, *J. Appl. Phys.*, *37*, 3203, doi:10.1063/1.1703185.

Buneman, O., et al. (1980), Principles and capabilities of 3-D, EM particle simulations, *J. Comput. Phys.*, *38*, 1–44, doi:10.1016/0021-9991(80)90010-8.

Buneman, O., et al. (1992), Solar wind-magnetosphere interaction as simulated by a 3-D EM particle code, *IEEE Trans. Plasma Sci.*, *20*(6), 810–816.

Cai, D. S., and O. Buneman (1992), Formation and stability of polarization sheaths of a cross-field beam, *Phys. Fluids B*, *4*, 1033, doi:10.1063/1.860226.

Cai, D. S., et al. (2001), Visualization and criticality of three-dimensional magnetic field topology in the magnetotail, *Earth Planets Space*, *53*, 1011.

Cai, D., et al. (2006a), Magnetotail field topology in a three-dimensional global particle simulation, *Plasma Phys. Controlled Fusion*, *48*(12B), 123, doi:10.1088/0741-3335/48/12B/S13.

Cai, D., X. Y. Yan, K.-I. Nishikawa, and B. Lembege (2006b), Particle entry into the inner magnetosphere during duskward IMF $B_y$: Global three-dimensional electromagnetic full particle simulations, *Geophys. Res. Lett.*, *33*, L12101, doi:10.1029/2005GL023520.

Cary, J. R., and I. Doxas (1993), An explicit symplectic integration scheme for plasma simulations, *J. Comput. Phys.*, *107*(1), 98–104, doi:10.1006/jcph.1993.1127.

Dorelli, J. C., A. Bhattacharjee, and J. Raeder (2007), Separator reconnection at Earth's dayside magnetopause under generic northward interplanetary magnetic field conditions, *J. Geophys. Res.*, *112*, A02202, doi:10.1029/2006JA011877.

Dungey, J. W. (1961), Interplanetary magnetic field and the auroral zones, *Phys. Rev. Lett.*, *6*(2), 47–48, doi:10.1103/PhysRevLett.6.47.

Guckenheim, J., and P. Holmes (1983), *Nonlinear Oscillation, Dynamical Systems and Bifurcation of Vector Fields*, Springer, New York.

Hesse, M., and K. Schindler (1988), A theoretical foundation of general magnetic reconnection, *J. Geophys. Res.*, *93*(A6), 5559–5567, doi:10.1029/JA093iA06p05559.

Hornig, G., and E. Priest (2003), Evolution of magnetic flux in an isolated reconnection process, *Phys. Plasmas*, *10*(7), 2712, doi:10.1063/1.1580120.

Lau, Y. T., and J. M. Finn (1990), Three-dimensional kinematic reconnection in the presence of field nulls and closed field lines, *Astrophys. J.*, *350*, 672–691, doi:10.1086/168419.

Lindman, E. L. (1975), Free-space boundary conditions for the time dependent wave equation, *J. Comput. Phys.*, *18*(1), 66–78, doi:10.1016/0021-9991(75)90102-3.

Linton, M. G., and S. K. Antiochos (2005), Magnetic flux tube reconnection: Tunneling versus slingshot, *Astrophys. J.*, *625*(1), 506–521, doi:10.1086/429585.

Nicolis, G., and I. Prigogine (1977), *Self-Organization in Nonequilibrium Systems*, John Wiley, New York.

Nicolis, G., and I. Prigogine (1989), *Exploring Complexity*, W. H. Freeman, New York.

Nishikawa, K. I. (1997), Particle entry into the magnetosphere with a southward interplanetary magnetic field studied by a three-dimensional electromagnetic particle code, *J. Geophys. Res.*, *102*(A8), 17,631–17,641, doi:10.1029/97JA00826.

Nishikawa, K.-I. (1998), Particle entry through reconnection grooves in the magnetopause with a dawnward IMF as simulated by a 3-D EM particle code, *Geophys. Res. Lett.*, *25*(10), 1609–1612, doi:10.1029/98GL01027.

Nishikawa, K. I., and S. Ohtani (2000a), Global particle simulation for a space weather model: Present and future, *IEEE Trans. Plasma Sci.*, *28*(6), 1991–2006, doi:10.1109/27.902227.

Nishikawa, K. I., and S. Ohtani (2000b), Evolution of thin current sheet with a southward interplanetary magnetic field studied by a three-dimensional electromagnetic particle code, *J. Geophys. Res.*, *105*(A6), 13,017–13,028, doi:10.1029/1999JA000215.

Pontin, D. I., et al. (2007a), Current sheet formation and nonideal behavior at three-dimensional magnetic null points, *Phys. Plasmas*, *14*, 052106, doi:10.1063/1.2722300.

Pontin, D. I., et al. (2007b), Current sheets at three-dimensional magnetic nulls: Effect of compressibility, *Phys. Plasmas*, *14*, 052109, doi:10.1063/1.2734949.

Priest, E., and T. Forbes (2000), *Magnetic Reconnection: MHD Theory and Applications*, Cambridge Univ. Press, Cambridge, U. K.

Prigogine, I. (1980), *From Being to Becoming*, W. H. Freeman, San Francisco, Calif.

Sattinger, D. H. (1973), *Topics in Stability and Bifurcation Theory*, Springer-Verlag, New York.

Schindler, K., et al. (1988), General magnetic reconnection, parallel electric fields, and helicity, *J. Geophys. Res.*, *93*, 5547–5557, doi:10.1029/JA093iA06p05547.

Schroer, A., et al. (1994), Numerical bifurcation study of a nonlinear current sheet model, *Phys. Plasmas*, *1*, 213, doi:10.1063/1.870554.

Strogatz, S. H. (1994), *Nonlinear Dynamics and Chaos*, Addison-Wesley, Reading, Mass.

Tobak, M., and D. J. Peake (1982), Topology of three-dimensional separated flows, *Annu. Rev. Fluid Mech.*, *14*(1), 61–85, doi:10.1146/annurev.fl.14.010182.000425.

Tricoche, X., et al. (2002), Topology tracking for the visualization of time-dependent two-dimensional flows, *Comput. Graph.*, *26*(2), 249–257, doi:10.1016/S0097-8493(02)00056-0.

Vasyliunas, V. M. (1984), Steady state aspects of magnetic field line merging, in *Magnetic Reconnection in Space and Laboratory Plasmas*, *Geophys. Monogr. Ser.*, vol. 30, pp. 25–31, AGU, Washington, D. C.

Villasenor, J., and O. Buneman (1992), Rigorous charge conservation for local electromagnetic field solvers, *Comput. Phys. Commun.*, *69*(2–3), 306–316, doi:10.1016/0010-4655(92)90169-Y.

Wiggins, S., et al. (2003), *Introduction to Applied Nonlinear Dynamical Systems and Chaos*, Springer, New York.

D. Cai, W. Tao, and X. Yan, Department of Computer Sciences, University of Tsukuba, 1-1-1 Ten-nou-dai, Tsukuba, Ibaraki 305-8573, Japan. (cai@aoi3.cs.tsukuba.ac.jp, twf@aoi3.cs.tsukuba.ac.jp, yxy@aoi3.cs.tsukuba.ac.jp)

B. Lembege, CETP, UVSQ, IPSL, 10-12 Avenue de l'Europe, F-78140 Velizy, France. (bertrand.lembege@cetp.ipsl.fr)

K.-I. Nishikawa, National Space Science and Technology Center, 320 Sparkman Drive, VP62, Huntsville, AL 35805, USA. (ken-ichi.nishikawa-1@nasa.gov)